

Plastics made from CO_2 in the air!

Showcasing research from Professor Licht's laboratory, at Direct Air Capture LLC, Carbon Corp, and the School of Chemistry, George Washington University, Washington DC, USA.

Polymer composites with carbon nanotubes made from CO_2

"The world on our shoulders" is a statue made from CO_2 in the air. Electrolysis transforms CO_2 to carbon nanotubes by the group's molten carbonate electrolysis C2CNT® decarbonization patented process and is 3D printed as a PLA-CNT composite. These carbon nanotube-plastic composites remove CO_2 and also use less polymer to achieve strength, thereby lowering the polymer's carbon footprint. C2CNT® is a DAC® (Direct Air Capture) and CCUS (Carbon Capture and Utilization) technology that has been scaled to industrial capacity at the Licht team's laboratories in Carbon Corp, Calgary, Canada (Carboncorp.org).

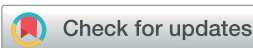
As featured in:



See Stuart Licht *et al.*,
RSC. Sustainability., 2024, 2, 2496.

COMMUNICATION

[View Article Online](#)
[View Journal](#) | [View Issue](#)



Cite this: *RSC Sustainability*, 2024, **2**, 2496

Received 12th May 2024
Accepted 3rd July 2024

DOI: 10.1039/d4su00234b

rsc.li/rscsus

Carbanogels are carbon nanotube (CNT) lattices formed by carbon capture and utilization molten carbonate electrolysis of CO₂. Higher tensile strength polymer composites with these CNTs from CO₂ are prepared with epoxies and thermoplastics. The composites use less polymer to achieve strength, thereby lowering the polymer's carbon footprint.

Introduction

Plastics are pervasively used and increasingly contribute to greenhouse gas emissions. However, the replacement of these materials with non-plastic materials would increase greenhouse gas emissions even further.¹ Plastic pollution is of growing concern, both in terms of the persistence of plastic in the environment and the large carbon footprint associated with its production.^{2,3} While continuing the pervasive societal use of plastics, one means to address both of these components of plastic pollution is to enhance plastic properties to enable lower usage, that is, to fulfill plastic functions, such as strength, hardness, or durability, while using less plastic.

Plastic composites prepared with graphene-based nanocomposites to enhance plastic properties, such as polymers with either carbon nanotubes (CNTs) or graphene, are of widespread interest.⁴⁻¹⁵ However, the commercial cost of synthesizing these graphene nanocarbons (GNCs) by chemical vapor deposition (CVD) has been high, and the CVD products carry a high carbon footprint.¹⁶ The current CVD costs of GNCs, such as CNTs, graphene, and carbon nano-onions, are in the range of \$1 million per tonne.

Reported polymer-GNC composites generally contain a maximum of 10% GNCs and can contain less than 0.1% GNC. Nevertheless, this low-level additive can confer substantial

Polymer composites with carbon nanotubes made from CO₂†

Gad Licht,^a Kyle Hofstetter^b and Stuart Licht^{ID *abc}

Sustainability spotlight

New sustainable plastics are demonstrated. Carbanogels are Carbon NanoTube (CNT) lattices formed by carbon capture and utilization molten carbonate electrolysis of CO₂. Carbanogels remove the greenhouse gas CO₂. Higher tensile strength polymer composites with these CNTs from CO₂ are prepared with epoxies and thermoplastics. The composites use less polymer to achieve strength, thereby lowering the polymer's carbon footprint.

improvements to the admixtures. The improvements are derived from the unusual enhancement of properties achieved by various GNCs, including CNTs with the highest tensile strength of all materials and excellent electronic, medical, structural, thermal, and catalytic properties for a range of manufacturing, medical, electronic, construction, military, transportation, and athletic applications.

Thermoplastics are often associated with materials requiring rigidity and include PLA (polylactic acid), PE (polyethylene), PP (polypropylene), PVC (polyvinyl chloride), ABS (acrylonitrile butadiene styrene), nylon, Teflon and polycarbonate or PC. PLA, as a thermoplastic, rather than a thermoset plastic, can be melted, heated, and cooled to resolidify and formed by molding, compression molding, machining, or 3D printing, and this capability is shared with all thermoplastics. The main limitation of PLA is its strength, which is a challenge that may be eliminated through the addition of carbon nanotubes. Historically, PVC-CNT and PLA-CNT composites were made by either dissolving plastic in solvent and dispersing the CNTs by sonication, then drying the admixtures, or melting plastic beads mixed with CNTs.^{4,5}

Alternatively, thermoset plastics are irreversibly cured by crosslinking in a permanent solid-state and are formed by chemical reactions. For example, as with thermoplastics, they can also be printed by 3D printing, but only *via* chemical reactions such as but not limited to photopolymerization or thermal chemical reactions. Prior to curing, thermoset plastic pre-cure components or components are available as liquids, which

^aDirect Air Capture LLC, A4 188 Triple Diamond Blvd, North Venice, FL 34275, USA.
E-mail: slicht@gwu.edu

^bCarbon Corp., 1035 26 St NE, Calgary, AB T2A 6K8, Canada

^cDept. of Chemistry, George Washington University, Washington DC 20052, USA

† Electronic supplementary information (ESI) available. See DOI: <https://doi.org/10.1039/d4su00234b>

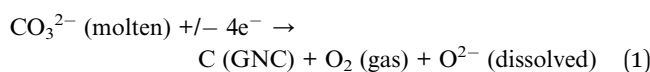


are often viscous or dense. Thermoset plastics are often resistant to higher temperatures and tend to decompose rather than melt at high temperatures.

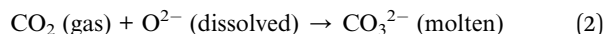
Common examples of thermoset plastics include epoxies (and epoxy resins), acrylics, phenolics, silicone (polysiloxanes), polyurethane (PU), polyimide, vulcanized rubber, Bakelite (polyoxybenzylmethyleneglycolanhydride), polycyclopentadiene (pDCPD), polyisocyanurate, polyester, polyurea, urea-formaldehyde, vinyl ester, cyanate, melamine, and polyester resins. The improvement of epoxy properties by the addition of CNTs has been of widespread interest.⁷⁻⁹ However, as with thermoplastic-CNT composites, these studies have only been conducted with high-carbon-footprint CVD-synthesized CNTs and have not focused on reducing the large carbon footprint associated with plastics.

This study presents a new low-cost plastic GNC composite in which the greenhouse gas carbon dioxide is consumed rather than emitted.

In 2009 (fundamental) and 2010 (experimental), the process of splitting CO_2 into carbon (C) and oxygen (O_2) *via* molten carbonate electrolysis emerged as a potential solution to address climate change.^{17,18} High-solubility molten pathways and the creative use of renewable energy-driven electrolysis decrease energy and cost. Subsequently, in 2015, it was demonstrated that during this electrolysis, the growth of transition metal nuclei leads to the direct conversion of CO_2 into pure CNTs¹⁹⁻²³ and other GNCs:



CO_2 chemically reacts with the electrolytic oxide formed through eqn (1) to renew CO_3^{2-} following eqn (2):



Combining eqn (1) and (2) yields a net decarbonization reaction:



During electrolysis, CO_2 is split into O_2 and GNCs. The latter grows as a matrix of intertwined graphene nanocarbons and electrolyte on the cathode as delineated in Fig. 1. The other graphene nanocarbons (GNCs) synthesized include helical, thin-walled, magnetic, and doped CNTs. Carbon nanobamboo, nano-pearl, and nano-tree morphologies as well as graphene.²⁴⁻³¹ Expanded details of this electrolysis process, the separation of the product from excess electrolyte, and product washing have recently been described and are detailed in the ESI.^{†32} This GNC/carbonate electrolyte cathode product mixture has been termed a carbanogel. The carbanogel consists of GNCs retaining interstitial electrolyte and is refined through the separation of the electrolyte.^{32,33} The CO_2 electrolysis parameters are manipulated to tailor the specific GNC produced by controlling the temperature, current density, and electrolyte composition. For example, a lower temperature (725°C) is commonly employed in the electrolytic formation of carbon nano-onions,²⁴ whereas a higher temperature range (750 to 770°C) is utilized for the electrolytic synthesis of CNTs.^{19-22,24-27,29}

This conversion of CO_2 offers an opportunity to harness greenhouse gases for the production of graphene-stabilized

CO₂ to Graphene Nanocarbon Material Processes (carbon nanotube example)

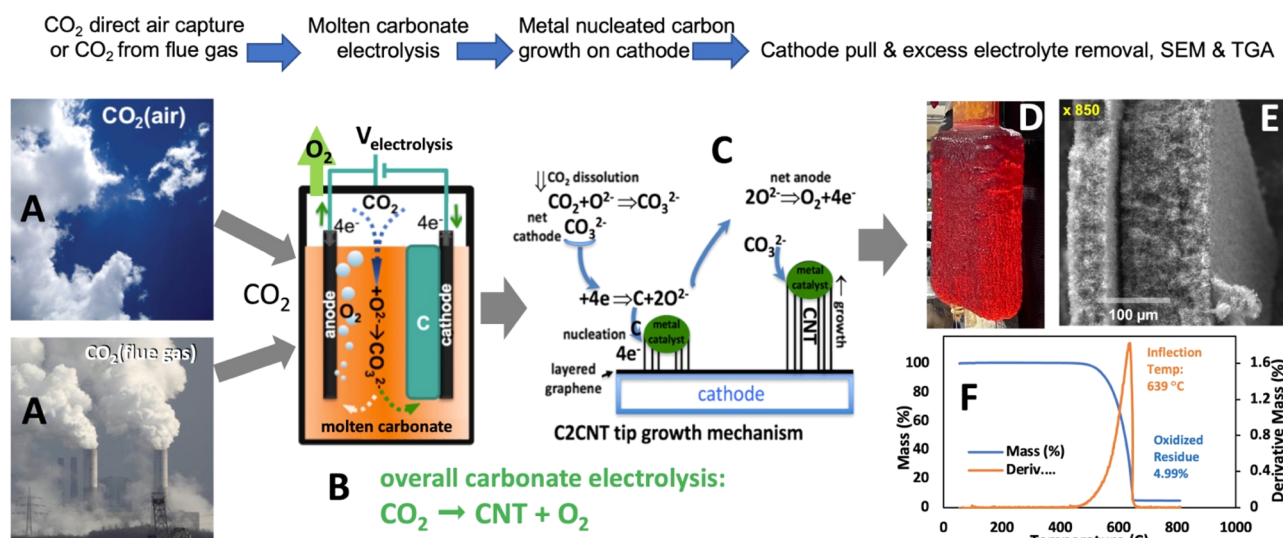


Fig. 1 The CO_2 to graphene nanocarbon material process (carbon nanotube example). (A) CO_2 is removed directly from air or flue gas (without preconcentration). (B) CO_2 is electrolyzed in molten carbonate. (C) The transition metal nucleated mechanism of electrolytic CO_2 transformation to CNT at the electrolysis cathode. (D) A pulled 1700 cm^2 cathode with deposited carbanogel (CNTs retaining interstitial electrolyte) subsequent to 18 hours electrolysis at 0.6 A cm^{-2} in 770°C Li_2CO_3 . (E) SEM of carbanogel subsequent to excess electrolyte removal & (F) TGA of CNT product.

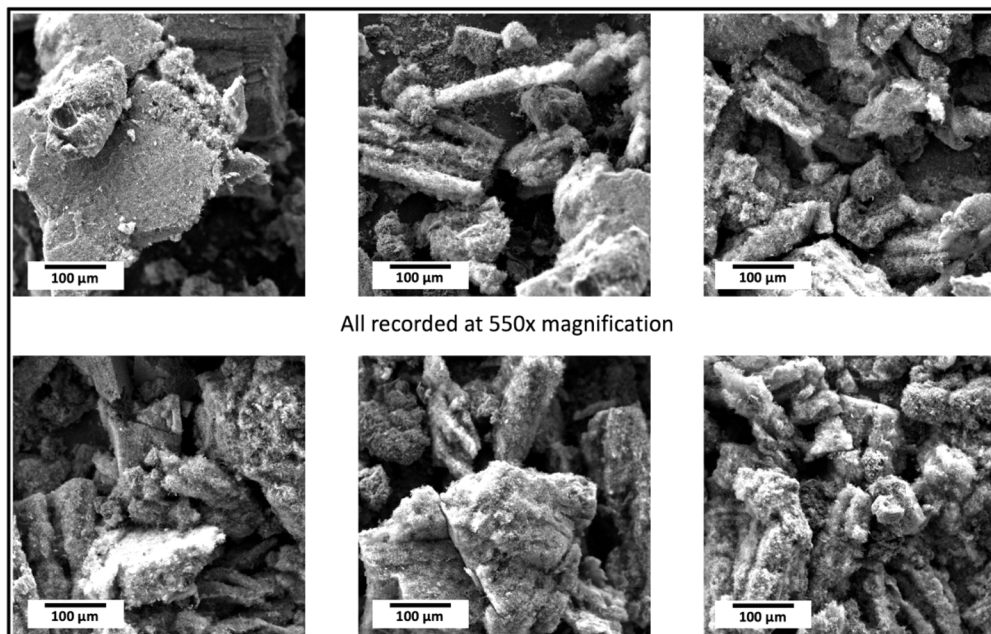


Fig. 2 The medium magnification of the SEM image shows the presence of macroscopic carbanogel particles.

nanocarbon allotropes, thereby aiding in climate change mitigation. Graphite, a macroscopic form of layered graphene, serves as a mineral with a geologic lifetime spanning hundreds of millions of years, providing a stability reference for graphene nanocarbon materials.

Experimental section

Carbanogel formation from CO₂

CO₂ was split in accord with eqn (1)–(3) in 770 °C molten Li₂CO₃ between a Muntz brass cathode and a 304 stainless steel anode at a constant electrolysis constant current density of 0.4 A cm⁻². The CO₂ source of the CNTs in this study is the (5% CO₂) flue gas from the Shepard Energy Centre natural gas power plant in Calgary, Canada. TGA of the product analyzed with a PerkinElmer STA 6000 TGA/DSC (Fig. 1F) showed that the product was more than 95% (less than 5% residual at 800 °C) pure and had an inflection temperature of 639 °C, which is indicative of a high graphene-like resistance to oxidative combustion. Acid purification further increases the CNT purity to >97%.

Microscopy of the carbanogel product

Scanning electron microscopy was conducted with a PHENOM Pro-X scanning electron microscope. SEM images of the products of this electrolysis at various magnifications. The medium-resolution SEM image (Fig. 2) shows that the GNC product consists of 30 to 300 μm-thick macroscopic particles. One benefit of isolating nanoparticles within a macroscopically dimensioned matrix as individual agglutinated, cohesive particles is that shipping these macroscopic larger particles mitigates respiratory hazards. Specifically, potential hazards sometimes associated

with shipping nanoscopic particles are avoided. Other benefits are that the structure provides an electrical and thermal conductive matrix, along with a highly porous framework for the accommodation of polymers, catalysts, or battery intercalation. At higher SEM magnification (Fig. 3), and over a range of magnifications (Fig. 4), the same electrolysis product shows that the individual carbanogel particles are composed of intertwined, high-purity CNTs. We've reported SEM, TEM, X-ray, and Raman, of the CNT and various GNC products as detailed in the ESI.†

Preparation and casting of epoxy–CNT composites

To prepare polymer–GNC composites, carbanogels can be used, as shown in Fig. 2, or crushed and mixed as separated CNTs with the polymer. One example of the former is the infusion of an elastomer within the carbanogel particle framework, which will be shown in a future study. In this study, the carbanogel was crushed and mixed as separated CNTs with various epoxies for tensile strength testing. Specifically, a desired weight of the washed, ground carbanogel was added to the epoxy. The weight was determined as a percentage compared to the total weight of the epoxy's resin and hardener.

After CO₂ electrolysis, the CNTs were added to the epoxy resin, mixed for 4 minutes at 65 rpm, and then sonicated for 3 minutes. Following sonication, the hardener was added, mixed at 65 rpm for 4 minutes, and then degassed for 3 minutes at 0.82 bar vacuum pressure. The samples were injected by syringe into ASTM casts and cured according to the manufacturer's guidelines at room temperature, or cured at 60 °C. The epoxies, either without or with CNTs were cast in ASTM D638 type V "dog bone" molds and removed for tensile strength testing.

Epoxies become jet black with the addition of CNTs. Examples are shown (Fig. 5) of dog bones prepared from one of the



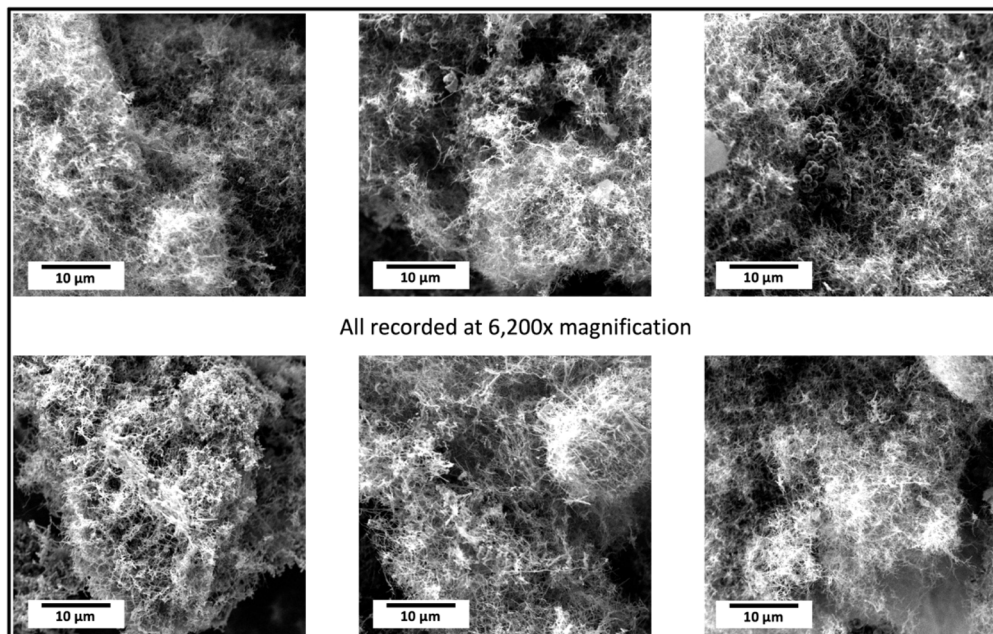


Fig. 3 High magnification of the SEM image shows the intertwined carbon nanotubes.

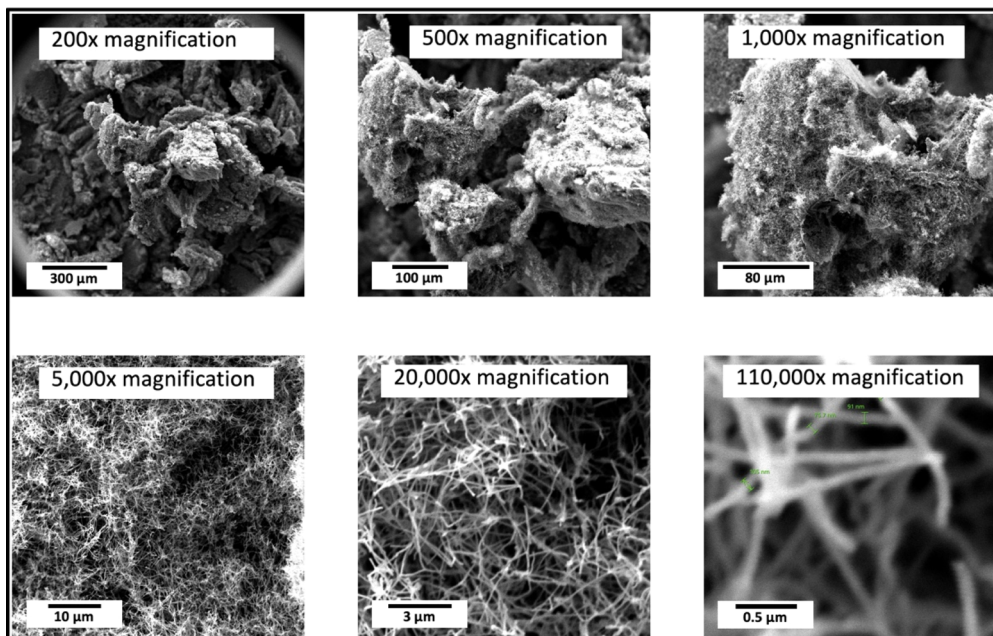


Fig. 4 A range of magnifications of the SEM product shows the individual carbon nanotubes and intertwined carbon nanotubes in the carbonogel product.

epoxies, Metlab, either pure or as a composite with 0.5 wt% CNTs made from CO₂.

CNT-epoxy composite tensile strength & hardness testing

The tensile strength of each dog bone sample was measured with an ETM-10kN Computer Controlled Electronic Universal Testing Production Machine.

A durometer hardness probe was acquired (Gain Express Digital Shore D Durometer with 0.5 step resolution), and the

hardness of the Metlab epoxy–CNT composites was measured with and without added CNTs.

Results and discussion

Polymer composite tensile strength with CNTs from CO₂

The mechanical properties of bisphenol-A (BPA) thermoset epoxies can be significantly improved with the addition of low levels of CNTs.^{34–37} Timber Cast Epoxy (Live Edge Timber Co.,





Fig. 5 Epoxy cast ASTM D638 type V dog bones used for tensile (stretch) strength testing. The casts on the left are with Metlab epoxy, and those on the right are cast with a composite of Metlab epoxy containing 0.5 wt% CNTs from CO_2 .

Quebec) is a deep-pour, 4 days-cured BPA epoxy. The resin is composed of 70–85 wt% chlorohydrin, bisphenol A copolymer/10–30 wt% *o*-cresol glycidyl ether, and 65–70 wt% trimethylolpropane poly(oxypropylene)triamine/35–40 wt% polypropylene glycol diamine hardener. The hardener was combined at a 1:2 by-weight ratio with the resin.^{38,39}

ASTM D628 type V casts were prepared with timber cast epoxy and either 0% (without added CNTs) or 0.5, 1, 1, 5, or 2.0 wt% CNTs from CO_2 by grinding carbanogels, as characterized by SEM (Fig. 2–4). CNTs were mixed by hand in the resin and then sonicated for 3 minutes. The hardener was then added, followed by another 4 minutes of hand mixing and 3 minutes of degassing the sample at 0.82 bar vacuum pressure to remove air bubbles. The mixed epoxy was added to the ASTM dog-bone molds and cured for 4 days at room temperature for tensile strength tests with an ETM-10kN Computer Controlled Electronic Universal Testing Production Instrument.

Compared to the tensile strength without the added carbanogel (Fig. 6), the tensile strength of the samples with 0.5, 1.0, 1.5, and 2.0 wt% ground carbanogels exhibited 2, 22, 30, and 23% relative increases in the measured tensile strength, respectively. For epoxy tensile strength-related applications, a 30% increase in the composite strength proportionally decreases the quantity of polymer needed, thereby decreasing the timber epoxy carbon footprint.

Varathane is a BPA (bisphenol A) epoxy that also reacts with epichlorohydrin (a 90 wt% epichlorohydrin-BPA) but with different support solvents and hardeners than the timber epoxy, and is intended for thin, high gloss coatings rather than for deep pours. It is dissolved as a resin in propylene carbonate (total < 15%). To form the thermoset epoxy, it is mixed with a hardener containing <40 wt% 4-nonylphenol, branched, <25 wt% polyoxypropylenediamine, <20 wt% trimethylpropylene triamine, 2-nonyl phenol, branched, 1-(2-aminoethyl) piperazine and <0.1 wt% 1-propene.⁴⁰

The Varathane samples were prepared with equal volumes of resin (10.87 g of resin and 8.83 g of hardener). Due to the lower viscosity of the Varathane hardener compared to the Timber hardener, rather than the resin, the hardener and sufficient CNTs were combined to produce the 0, 0.05, 1, 1.5, or 2 wt% CNT composites. The hardener CNT was mixed by hand and

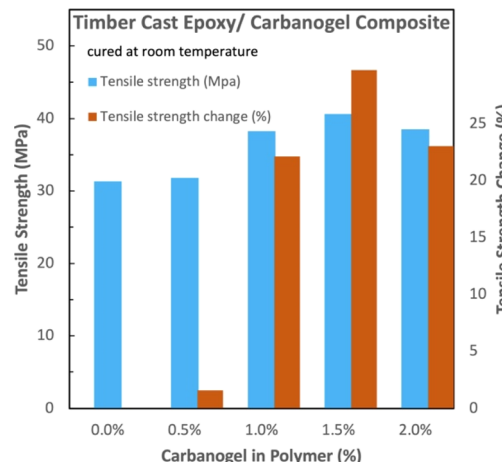


Fig. 6 Comparison of the absolute and relative tensile strengths of the timber epoxy with and without carbanogel CNTs from CO_2 .

then sonicated for 3 minutes. The resin was added, and the mixture was hand mixed for 3 more minutes, degassed for 3 minutes, cast in dog bone molds, cured for 4 days at room temperature, and tested for tensile strength.

Compared to the Timber epoxy, the Varathane-CNT composites exhibit greater relative tensile strength (Fig. 7), with a 55% increase in strength for the 1 wt% CNT composite. Hence, the same tensile strength of Varathane epoxy prepared with the 1 wt% Varathane-CNT epoxy requires 1/1.55 (~64%) less polymer, decreasing the Varathane epoxy carbon footprint.

Jetset-Metlab epoxy is a fast-curing BPA epoxy. The resin contains 80–90 wt% propane, 2,2-bis[*p*-(2,3-epoxypropoxy) phenol], polymers and 10–20 wt% alkyl(C12–14) glycidyl ether. The hardener is composed of 60–70 wt% diethylenetriamine, 30–40 wt% bisphenol A, <0.8% aminoethylpiperazine, and <0.2% ethylenediamine.^{41,42} A total of 27.1 g of resin is used with each 2.8 g of hardener. CNTs from CO_2 are mixed with the resin and combined with the hardener and prepared for the dog bone tensile strength test as described for the Timber epoxy and

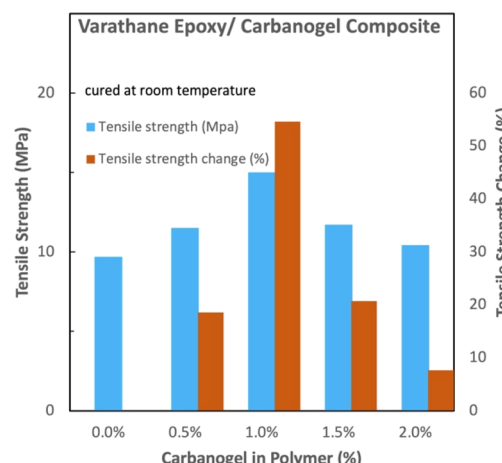


Fig. 7 Comparison of the absolute and relative tensile strengths of Varathane epoxy with and without carbanogel CNTs from CO_2 .



cured for a longer period of time, 5 days at room temperature, to reach the curing limit.

The tensile strength of the room-temperature-cured Jetset-Metlab-CNT composites (Fig. 8) exhibited a maximal tensile strength increase of 48% at 1.0 to 1.5 wt% carbanogel in the polymer.

Interestingly, this Metlab composite exhibits greater strength increases at low (0.5 wt%) carbanogel CNT additions, and as noted for the other epoxies, the increase in strength is equivalent to a decrease in the needed polymer, resulting in a decrease of the carbon footprint for each of the three composites of epoxy-CNTs from the CO_2 .

A durometer hardness probe with 0.5 step resolution was used to measure the hardness of the Jetset-Metlab epoxy samples prepared with and without added CNTs (Fig. 9). The magnitude of the hardness increased from 74 without CNTs increases to a maximum value of ~ 78 in the same CNT concentration range (1 to 1.5 wt%) as the maximum measured tensile strength with added CNT concentration domain in Fig. 8. Beyond the percolation threshold concentration of approximately 2% CNT, polymer conductivity increases are also anticipated.

The conditions of curing will affect the epoxy strength. Jetset-Metlab epoxy was also prepared with an alternative (60 °C, rather than room temperature) cure and over a wider range of carbanogel concentrations (Fig. 10). In the figure, curing at a higher temperature increases the tensile strength, either without or with the added CNTs. With the Jetset-Metlab-composite, the trend of enhanced tensile strength with added CNTs continued under lower CNT conditions, albeit to a lesser extent.

Thermoplastic-carbanogel tensile strength increase

As a preliminary low-carbon footprint thermoplastic study, plastic-carbanogel high-quality composites were made with thermoplastic PLA or ABS rather than thermoset epoxies by extrusion. Thermoplastic carbon nanotubes have been previously studied,^{43–48} albeit without CNTs made from CO_2 . This

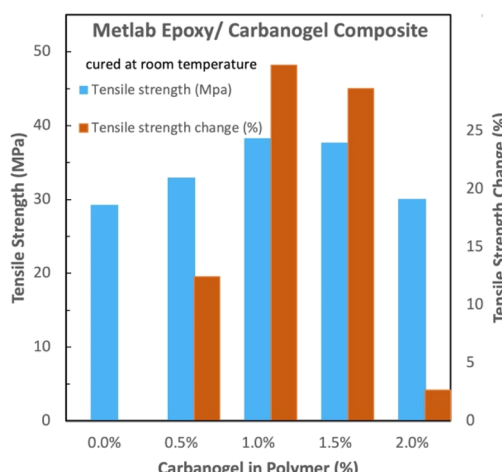


Fig. 8 Room-temperature-cured Metlab epoxy. Comparison of the absolute and relative tensile strengths with and without carbanogel CNTs from CO_2 .

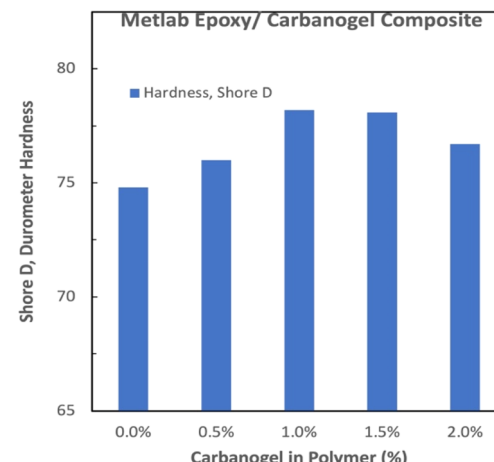


Fig. 9 The measured hardness of room Metlab epoxy with and without carbanogel CNTs from CO_2 .

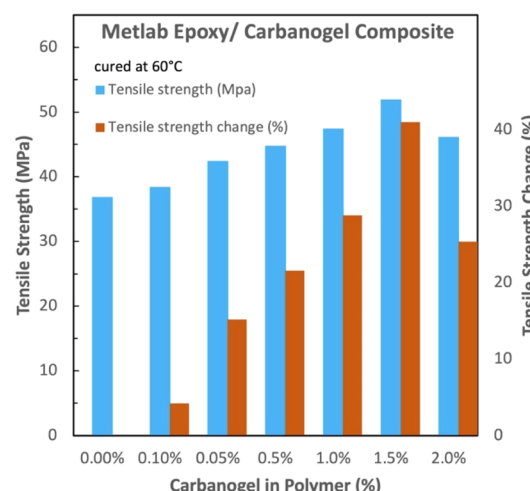


Fig. 10 60 °C cured Metlab epoxy. Comparison of the absolute and relative tensile strengths with and without carbanogel CNTs from CO_2 .

preliminary communication focuses on the PLA–carbanogel composites. PLA Plus pellets (3DXTech) beads were mixed with or without 1% of the (uncrushed carbanogel) and fed at 220 °C through a Felfil Evo Filament Extruder, exiting through the filament nozzles for cooling, hardening, and fiber collection by a Felfil Evo Spooler. The filament was then fed through a Felfil plastic shredder, and the shorter filaments looped back into the extruder. This process was repeated five times to ensure effective PLA/CNT mixing. The finished fiber was crosshatch printed with a Creality Ender 3D printer to form the ASTM D638 V dog bones for tensile strength testing. PLA–CNTs from the CO_2 composites (0, 2, 4, 6, or 8 wt%) were prepared, and the 6 wt% composite exhibited a maximum 65% increase in textural strength.

Incentivized carbon mitigation

An equivalent performance with less plastic equates to a decrease in the plastic footprint. The current commercial

costs for GNCs, such as those for CNTs, nano-onions, and graphene, are high due to the high energy, material, and energy costs, and high carbon footprint of CVD production. In comparison, the only reactant involved in the C2CNT (CO_2 to carbon nanomaterial technology) formation of GNCs is CO_2 , and the electrolysis energy needed to split and transform CO_2 to GNCs ranges from 0.8 to 2 V.⁴⁹ Hence, C2NCT GNC costs are up to 3 orders of magnitude lower than those of CVD, and in bulk are on the order of \$1000 per ton. C2CNT GNC costs and production components are comparable to those of another industrial electrolytic process that splits aluminum oxide to produce commercial grade aluminum metal.²⁰ C2CNT costs decrease further when solar and wind provide alternative energy sources.^{50–57} In comparison, the plastic material and resin price index has reached \$300–\$400 per tonne over the past 3 years.⁵⁸ Hence, a 1% by weight C2CNT addition of GNC that adds less than \$30 to \$40 per ton cost to plastics will be offset if substantial (>10%) mechanical, thermal, or electrical improvements are achieved. Similarly, the carbon footprint is reduced when less plastic is used to achieve the desired property.

Conclusions

Polymer composites with carbon nanotubes made from CO_2 provide a path for lowering plastic pollution and the carbon footprint of plastics. Carbanogels, which form during the electrolysis of CO_2 in molten carbonates, provide highly porous matrices of graphene nanocarbons, such as carbon nanotubes.

Low-level carbanogels can be combined with plastics to form polymer–carbanogel composites, including polymer–CNT composites. Carbon nanotubes have intrinsic properties of high strength and high thermal and electrical conductivity, and in plastic composites, these properties can improve the characteristics of plastics. A few percent addition of these carbanogel CNTs can increase the tensile strength of both thermoset epoxies and thermoplastics. In several cases, this strength enhancement is greater than 50%. The need for less plastic to achieve the same strength lowers the polymer's carbon footprint. Increases in polymer hardness and conductivity can also be anticipated with the addition of CNTs produced CO_2 . The greenhouse gas CO_2 provides a low-cost reactant to form graphene nanocarbon composite additives by electrolysis. Combined with the low cost of electrolysis, this results in an expensive decarbonization process to incentivize lower CO_2 emissions associated with the pervasive use of plastics.

Data availability

The data supporting this article have been included as part of the ESI.†

Conflicts of interest

There are no conflicts to declare.

Acknowledgements

We are grateful to Moolod Nasirikheirabadi, Stefan Feldrihan, and Amirreza Badri of Carbon Corp for their experimental contributions.

Notes and references

- 1 F. Meng, N. Brandao and J. M. Cullen, Replacing Plastics with Alternatives Is Worse for Greenhouse Gas Emissions in Most Cases, *Environ. Sci. Technol.*, 2024, **58**, 2716–2727, DOI: [10.1021/acs.est.3c05191](https://doi.org/10.1021/acs.est.3c05191).
- 2 P. Stegmann, V. Daioglou, M. Lando, D. P. van Vuuren and M. Junginger, Plastic Futures and the CO_2 emissions, *Nature*, 2022, **612**, 272–276, DOI: [10.1038/s41586-022-05422-5](https://doi.org/10.1038/s41586-022-05422-5).
- 3 X.-F. Wei, W. Yang and M. S. Hedengvist, Plastic pollution amplified by a warming climate, *Nat. Commun.*, 2024, **15**, 2052, DOI: [10.1038/s41467-024-46127-9](https://doi.org/10.1038/s41467-024-46127-9).
- 4 J. Y. D. Varela, L. G. B. Jurado, I. O. Armendáriz, C. A. M. Pérez and C. C. González, The role of multiwalled carbon nanotubes in enhancing the hydrolysis and thermal stability of PLA, *Sci. Rep.*, 2024, **14**, 8405, DOI: [10.1038/s41598-024-58755-8](https://doi.org/10.1038/s41598-024-58755-8).
- 5 K. Skórczewska, S. Wilczewski and K. Lewandowski, Multiscale Carbon Fiber–Carbon Nanotube Composites of Poly(Vinyl Chloride)—An Evaluation of Their Properties and Structure, *Molecules*, 2024, **29**, 1479, DOI: [10.3390/molecules29071479](https://doi.org/10.3390/molecules29071479).
- 6 T. P. Dyachkova, Y. A. Khan, E. A. Burakova, E. V. Galunin, G. N. Shigabaeva, D. N. Stolbov, G. A. Titov, N. A. Chapaksov and A. G. Tkachev, Characteristics of Epoxy Composites Containing Carbon Nanotubes/Graphene Mixtures, *Polymers*, 2023, **15**, 15061476, DOI: [10.3390/polym15061476](https://doi.org/10.3390/polym15061476).
- 7 N. P. Singh, V. K. Gupta and A. P. Singh, Graphene and carbon nanotube reinforced epoxy nanocomposites - A review, *Polymer*, 2019, **180**, 121724, DOI: [10.1016/j.polymer.2019.121724](https://doi.org/10.1016/j.polymer.2019.121724).
- 8 J. C. Long, H. Zhan, G. Wu, Y. Zhang and J. N. Wang, High-strength carbon nanotube/epoxy resin composite film from a controllable cross-linking reaction, *Composites, Part A*, 2021, **146**, 106490, DOI: [10.1016/j.compositesa.2021.106490](https://doi.org/10.1016/j.compositesa.2021.106490).
- 9 A. Hu and H. Hong, Review on Material Performance of Carbon Nanotube-Modified Polymeric Nanocomposites, *Recent Prog. Mater.*, 2023, **5**, 2303031, DOI: [10.21926/rpm.2303031](https://doi.org/10.21926/rpm.2303031).
- 10 C. L. Brito, J. V. Silva, R. V. Gonzaga, M. A. La-Sclea, J. Giarolla and E. I. Ferreira, A Review on Carbon Nanotubes Family of Nanomaterials and Their Health Field, *ACS Omega*, 2024, **9**, 8687–8708, DOI: [10.1021/acsomega.3c08824](https://doi.org/10.1021/acsomega.3c08824).
- 11 M. Choudhary, A. Sharma, S. Raj, M. T. H. Sultan, D. Hui and A. U. M. Shah, Contemporary review on carbon nanotube (CNT) composites and their impact on multifarious applications, *Nanotechnol. Rev.*, 2022, **11**, 2632–2660, DOI: [10.1515/ntrev-2022-0146](https://doi.org/10.1515/ntrev-2022-0146).



12 P. Parnia, A Short Review on - Recent Advances in the Use of Carbon Nanotubes in Additive Manufacturing of Polymer Matrix Composites, *Macromol. Symp.*, 2022, **405**, 2100339, DOI: [10.1002/masy.202100339](https://doi.org/10.1002/masy.202100339).

13 N. M. Nurazzi, M. R. M. Asyraf and E. S. Zainudin, Mechanical Performance and Applications of CNTs Reinforced Polymer Composites—A Review, *nanomaterials*, 2021, **11**, 2186, DOI: [10.3390/nano11092186](https://doi.org/10.3390/nano11092186).

14 A. Iqbal, A. Saeed and A. Ul-Hamid, A review featuring the fundamentals and advancements of polymer/CNT nanocomposite application in aerospace industry, *Polym. Bull.*, 2020, **78**, 539–557, DOI: [10.1007/s00289-019-03096-0](https://doi.org/10.1007/s00289-019-03096-0).

15 S. K. Soni, T. Thomas and V. R. Kar, A Comprehensive Review on CNTs and CNT-Reinforced Composites - Syntheses, Characteristics and Applications, *Mater. Today Commun.*, 2020, **25**, 101546, DOI: [10.1016/j.mtcomm.2020.101546](https://doi.org/10.1016/j.mtcomm.2020.101546).

16 K. A. Shah and B. A. Tali, Synthesis of carbon nanotubes by catalytic chemical vapor deposition: A review on carbon sources, catalysts and substrates, *Mater. Sci. Semicond. Process.*, 2016, **41**, 67–82, DOI: [10.1016/j.mssp.2015.08.013](https://doi.org/10.1016/j.mssp.2015.08.013).

17 J. Ren, F.-F. Li, J. Lau, L. Gonzalez-Urbina and S. Licht, One-pot synthesis of carbon nanofibers from CO₂, *Nano Lett.*, 2015, **15**, 6142–6148, DOI: [10.1021/jp9044644](https://doi.org/10.1021/jp9044644).

18 J. Ren and S. Licht, Tracking airborne CO₂ mitigation and low cost transformation into valuable carbon nanotubes, *Sci. Rep.*, 2016, **6**, 27760, DOI: [10.1038/srep27760](https://doi.org/10.1038/srep27760).

19 J. Ren, M. Johnson, R. Singhal and S. Licht, Transformation of the greenhouse gas CO₂ by molten electrolysis into a wide controlled selection of carbon nanotubes, *J. CO₂ Util.*, 2017, **18**, 335–344, DOI: [10.1016/j.jcou.2017.02.005](https://doi.org/10.1016/j.jcou.2017.02.005).

20 M. Johnson, J. Ren, M. Lefler, G. Licht, J. Vicini and S. Licht, Data on SEM, TEM and Raman spectra of doped, and wool carbon nanotubes made directly from CO₂ by molten electrolysis, *Data Brief*, 2017, **14**, 592–606.

21 M. Johnson, J. Ren, M. Lefler, G. Licht, J. V. X. Liu and S. Licht, Carbon nanotube wools made directly from CO₂ by molten electrolysis: Value driven pathways to carbon dioxide greenhouse gas mitigation, *Mater. Today Energy*, 2017, **5**, 230–236, DOI: [10.1016/j.mtener.2017.07.003](https://doi.org/10.1016/j.mtener.2017.07.003).

22 X. Wang, X. Liu, G. Licht, B. Wang and S. Licht, Exploration of alkali cation variation on the synthesis of carbon nanotubes by electrolysis of CO₂ in molten carbonates, *J. CO₂ Util.*, 2019, **18**, 303–312, DOI: [10.1016/j.jcou.2019.07.007](https://doi.org/10.1016/j.jcou.2019.07.007).

23 X. Liu, G. Licht and S. Licht, Controlled Transition Metal Nucleated Growth of Carbon Nanotubes by Molten Electrolysis of CO₂, *Catalysts*, 2022, **12**, 137, DOI: [10.3390/catal12020137](https://doi.org/10.3390/catal12020137).

24 X. Liu, J. Ren, G. Licht, X. Wang and S. Licht, Carbon nano-onions made directly from CO₂ by molten electrolysis for greenhouse gas mitigation, *Adv. Sustainable Syst.*, 2019, **3**, 1900056, DOI: [10.1002/adsu.201900056](https://doi.org/10.1002/adsu.201900056).

25 X. Wang, X. Liu, G. Licht and S. Licht, Calcium metaborate induced thin walled carbon nanotube syntheses from CO₂ by molten carbonate electrolysis, *Sci. Rep.*, 2020, **10**, 15146, DOI: [10.1038/s41598-020-71644-0](https://doi.org/10.1038/s41598-020-71644-0).

26 X. Wang, F. Sharif, X. Liu, G. Licht, M. Lefler and S. Licht, Magnetic carbon nanotubes: Carbide nucleated electrochemical growth of ferromagnetic CNTs, *J. CO₂ Util.*, 2020, **40**, 101218, DOI: [10.1016/j.jcou.2020.101218](https://doi.org/10.1016/j.jcou.2020.101218).

27 G. Licht, X. Wang, X. Liu and S. Licht, CO₂ Utilization by Electrolytic Splitting to Carbon Nanotubes in Non-Lithiated, Cost-Effective, Molten Carbonate Electrolytes, *Adv. Sustainable Syst.*, 2022, 10084, DOI: [10.1002/adsu.202100481](https://doi.org/10.1002/adsu.202100481).

28 X. Wang, G. Licht, X. Liu and S. Licht, One pot facile transformation of CO₂ to an unusual 3-D nan-scaffold morphology of carbon, *Sci. Rep.*, 2020, **10**, 21518, DOI: [10.1038/s41598-020-78258-6](https://doi.org/10.1038/s41598-020-78258-6).

29 X. Liu, G. Licht and S. Licht, The green synthesis of exceptional braided, helical carbon nanotubes and nanospiral platelets made directly from CO₂, *Mater. Today Chem.*, 2021, **22**, 100529, DOI: [10.1016/j.mtchem.2021.100529](https://doi.org/10.1016/j.mtchem.2021.100529).

30 X. Liu, X. Wang, G. Licht and S. Licht, Transformation of the greenhouse gas carbon dioxide to graphene, *J. CO₂ Util.*, 2020, **236**, 288–294, DOI: [10.1016/j.jcou.2019.11.019](https://doi.org/10.1016/j.jcou.2019.11.019).

31 X. Liu, G. Licht, X. Wang and S. Licht, Controlled Growth of Unusual Nanocarbon Allotropes by Molten Electrolysis of CO₂, *Catalysts*, 2022, **12**, 137, DOI: [10.3390/catal12020125](https://doi.org/10.3390/catal12020125).

32 G. Licht, K. Hofstetter and S. Licht, Separation of Molten Electrolyte from the Graphene Nanocarbon Product Subsequent to Electrolytic CO₂ Capture, *Decarbon*, 2024, **4**, 100044, DOI: [10.1016/j.decarb.2024.100044](https://doi.org/10.1016/j.decarb.2024.100044).

33 X. Wang, G. Licht and S. Licht, Green and scalable separation and purification of carbon materials in molten salt by efficient high-temperature press filtration, *Sep. Purif. Technol.*, 2021, **244**, 117719, DOI: [10.1016/j.seppur.2020.117719](https://doi.org/10.1016/j.seppur.2020.117719).

34 S. A. Bansal, V. Khanna, T. A. P. Singh and S. Kumar, Bisphenol-A–Carbon Nanotube Nanocomposite: Interfacial DFT Prediction and Experimental Strength Testing, *Langmuir*, 2023, **39**, 1051–1060, DOI: [10.1021/acs.langmuir.2c02723](https://doi.org/10.1021/acs.langmuir.2c02723).

35 S. A. Bansal, V. Khanna, T. A. P. Singh and S. Kumar, Small percentage reinforcement of carbon nanotubes (CNTs) in epoxy(bisphenol-A) for enhanced mechanical performance, *Mater. Today: Proc.*, 2022, **61**, 275–279, DOI: [10.1016/j.matpr.2021.09.225](https://doi.org/10.1016/j.matpr.2021.09.225).

36 B. Du, K. Yang, R. Luo, H. Lin, S. Zhou and Y. Lu, Reinforcement of Bisphenol-A epoxy resin nanocomposites with noncovalent functionalized and physical adsorption modified CNTs, *Mater. Res. Express*, 2019, **6**, 105623, DOI: [10.1088/2053-1591/ab3fe6](https://doi.org/10.1088/2053-1591/ab3fe6).

37 S. A. Awad, C. M. Fellows and S. S. Mahini, Evaluation of bisphenol A-based epoxy resin containing multiwalled carbon nanotubes to improve resistance to degradation, *J. Compos. Mater.*, 2018, **53**, 2993–3003, DOI: [10.1177/0021998318816784](https://doi.org/10.1177/0021998318816784).

38 Timber Cast Safety Data Sheet Part A, <https://go.rockler.com/msds/Timber-Cast-Casting-Epoxy-SDS1.PDF>, accessed May 10, 2024.



39 Timber Cast Safety Data Sheet Part B, [https://go.rockler.com/msds/Timber-Cast-Casting-Epoxy-SDS-2.PDF](https://go.rockler.com/msds/Timber-Cast-Casting-Epoxy-SDS-https://go.rockler.com/msds/Timber-Cast-Casting-Epoxy-SDS-2.PDF), accessed May 10, 2024.

40 Varane Safety Data Sheet, Rust-oleum corporation, accessed May 10, 2024.

41 Jetset Metlab Safety Data Sheet hardener, https://www.metlabcorp.com/files/resources/JETSET_HARDENER_1.pdf, accessed May 11, 2024.

42 Jetset Metlab Safety Data Sheet resin, https://www.metlabcorp.com/files/resources/jetset_EPOXY_RESIN_NEW.pdf, accessed May 11, 2024, ibid, https://metlabcorp.com/files/resources/JETSET_HARDENER_1.pdf.

43 N. Salah, A. M. Alfawzan, A. Saeed, A. Alsharie and W. Allafi, Effective reinforcements for thermoplastics based on carbon nanotubes of oil fly ash, *Sci. Rep.*, 2019, **9**, 20288, DOI: [10.1038/s41598-019-56777-1](https://doi.org/10.1038/s41598-019-56777-1).

44 M. M. Younus, H. M. Naguib, M. Fekry and M. A. Elsawy, Pushing the limits of PLA by exploring the power of MWCNTs in enhancing thermal, mechanical properties, and weathering resistance, *Sci. Rep.*, 2023, **13**, 16599, DOI: [10.1038/s41598-023-43660-3](https://doi.org/10.1038/s41598-023-43660-3).

45 C. Goncalves, I. C. Goncalves, F. D. Magalhaes and A. M. Pinto, Poly(lactic acid) Composites Containing Carbon-Based Nanomaterials: A Review, *polymers*, 2017, **9**, 269, DOI: [10.3390/polym9070269](https://doi.org/10.3390/polym9070269).

46 A. H. Maleki and A. Zolfaghari, Investigation of electrical, electromagnetic interference shielding and tensile properties of 3D-printed acrylonitrile butadiene styrene/carbon nanotube composites, *J. Thermoplast. Compos. Mater.*, 2023, **37**, 2409–2424, DOI: [10.1177/08927057231216736](https://doi.org/10.1177/08927057231216736).

47 S. Dul, L. Fambri and A. Pegoretti, Filaments Production and Fused Deposition Modeling of ABS/Carbon Nanotubes Composites, *Nanomaterials*, 2018, **8**, 40, DOI: [10.3390/nano8010049](https://doi.org/10.3390/nano8010049).

48 J. Ren, J. Lau, M. Lefler and S. Licht, The minimum electrolytic energy needed to convert carbon dioxide to carbon by electrolysis in carbonate melts, *J. Phys. Chem. C*, 2015, **119**, 23342–23349, DOI: [10.1021/acs.jpcc.5b07026](https://doi.org/10.1021/acs.jpcc.5b07026).

49 S. Licht, STEP (solar thermal electrochemical photo) generation of energetic molecules: A solar chemical process to end anthropogenic global warming, *J. Phys. Chem. C*, 2009, **113**, 16283–16292, DOI: [10.1021/jp9044644](https://doi.org/10.1021/jp9044644).

50 S. Licht, B. Wang, S. Ghosh, H. Ayub, D. Jiang and J. Ganley, New solar carbon capture process: STEP carbon capture, *J. Phys. Chem. Lett.*, 2010, **1**, 2363–2368, DOI: [10.1021/jz100829s](https://doi.org/10.1021/jz100829s).

51 S. Licht, B. Wang, T. Soga and M. Umeno, Light invariant, efficient, multiple band gap AlGaAs/Si/metal hydride solar cell, *Appl. Phys. Lett.*, 1999, **74**, 4055–4057, DOI: [10.1063/1.123259](https://doi.org/10.1063/1.123259).

52 S. Licht, L. Halperin, M. Kalina, M. Zidman and N. Halperin, Electrochemical potential tuned solar water splitting, *Chem. Commun.*, 2003, **2003**, 3006–3007, DOI: [10.1039/B309397B](https://doi.org/10.1039/B309397B).

53 S. Licht, Thermochemical solar hydrogen generation, *Chem. Commun.*, 2005, **2005**, 4635–4646, DOI: [10.1039/B508466K](https://doi.org/10.1039/B508466K).

54 S. Licht, N. Myung and Y. Sun, A light addressable photoelectrochemical cyanide sensor, *Anal. Chem.*, 1996, **68**, 954–959, DOI: [10.1021/ac9507449](https://doi.org/10.1021/ac9507449).

55 S. Licht and B. Wang, High solubility pathway for the carbon dioxide free production of iron, High solubility pathway for the carbon dioxide free production of iron, *Chem. Commun.*, 2010, **46**, 7004–7006, DOI: [10.1039/C0CC01594F](https://doi.org/10.1039/C0CC01594F).

56 S. Licht, O. Chitayat, H. Bergmann, A. Dick, H. Ayub and S. Ghosh, Efficient STEP (solar thermal electrochemical photo) production of hydrogen—an economic assessment, *Int. J. Hydrogen Energy*, 2010, **35**, 10867–10882, DOI: [10.1016/j.ijhydene.2010.07.028](https://doi.org/10.1016/j.ijhydene.2010.07.028).

57 J. Ren, A. Yu, P. Peng, M. Lefler, F.-F. Li and S. Licht, Recent advances in solar thermal electrochemical process (STEP) for carbon neutral products and high value nanocarbons, *Acc. Chem. Res.*, 2019, **52**, 3177–3187, DOI: [10.1021/acs.accounts.9b00405](https://doi.org/10.1021/acs.accounts.9b00405).

58 US Producer Price Index: Plastics Material and Resins Manufacturing, https://ycharts.com/indicators/us_producer_price_index_plastics_material_and_resins_manufacturing#:~:text=USProducerPriceIndexAPlasticsMaterialandResinsManufacturingis,5.81fromoneyearago, accessed May 9, 2024.

